Published in final edited form as:
Neuroscience. 2006 August 25; 141(2): 621–636. doi:10.1016/j.neuroscience.2006.04.069.

Nucleus- and species-specific properties of the slow (<1 Hz) sleep oscillation in thalamocortical neurons

Linyan Zhu[*], **Kate L. Blethyn**, **David W. Cope**, **Vera Tsomaia**, **Vincenzo Crunelli**, and **Stuart W. Hughes**
School of Biosciences, Cardiff University, Museum Avenue, Cardiff CF10 3US, UK.

Abstract

The slow (<1 Hz) rhythm is an EEG hallmark of resting sleep. In thalamocortical (TC) neurons this rhythm correlates with a slow (<1 Hz) oscillation comprising recurring UP and DOWN membrane potential states. Recently, we showed that metabotropic glutamate receptor (mGluR) activation brings about an intrinsic slow oscillation in thalamocortical (TC) neurons of the cat dorsal lateral geniculate nucleus (LGN) *in vitro* which is identical to that observed *in vivo*. The aim of this study was to further assess the properties of this oscillation and compare them with those observed in TC neurons of three other thalamic nuclei in the cat (ventrobasal complex, VB; medial geniculate body, MGB; ventral lateral nucleus, VL) and two thalamic nuclei in rats and mice (LGN and VB). Slow oscillations were evident in all of these additional structures and shared several basic properties including, i) the stereotypical, rhythmic alternation between distinct UP and DOWN states with the UP state always commencing with a low-threshold Ca^{2+} potential (LTCP), and ii) an inverse relationship between frequency and injected current so that slow oscillations always increase in frequency with hyperpolarization, often culminating in delta (δ) activity at ~1-4 Hz. However, beyond these common properties there were important differences in expression between different nuclei. Most notably, 44% of slow oscillations in the cat LGN possessed UP states that comprised sustained tonic firing and/or high-threshold (HT) bursting. In contrast, slow oscillations in cat VB, MGB and VL TC neurons exhibited such UP states in only 16%, 11% and 10% of cases, respectively, whereas slow oscillations in the LGN and VB of rats and mice did so in <12% of cases. Thus, the slow oscillation is a common feature of TC neurons that displays clear species- and nuclei-related differences. The potential functional significance of these results is discussed.

Keywords

EEG; delta waves; T-type calcium channels; metabotropic glutamate receptor

During resting sleep the human EEG exhibits a distinctive slow (<1 Hz) rhythm (Amzica and Steriade, 1997; see also Achermann and Borbely, 1997). This slow rhythm is also evident during natural sleep in cats (Amzica and Steriade, 1998, Steriade et al., 2001, Timofeev et al., 2001), rats (Pinault et al., 2001) and mice (Lee et al., 2004), and is prominent in the EEG of cats maintained under either urethane or ketamine/xylazine anaesthesia (Steriade et al., 1993a,b,c). The presence of the slow rhythm in cats during general anaesthesia has greatly facilitated the *in vivo* investigation of its cellular components. Specifically, studies exploiting this fact have revealed that in both cortical and

Correspondence: S.W. Hughes, School of Biosciences, Cardiff University, Museum Avenue, Cardiff CF10 3US, UK. Tel.: +44 (0)29 20879113, Fax.: +44 (0)29 20874986 HughesSW@Cardiff.ac.uk.
[*]Present address: Department of Physiology, Zhongshan Medical College, Sun Yatsen University, Guangzhou 510080, Peoples Republic of China.

Europe PMC Funders Author Manuscripts

thalamic neurons, the slow rhythm corresponds to a slow (<1 Hz) membrane potential oscillation consisting of distinct UP and DOWN states (Steriade et al., 1993a,b,c). In cortical neurons, these UP and DOWN states seem to be largely sculpted by alternating periods of intense synaptic barrages and disfacilitation, respectively (Steriade et al., 1993a,b; Sanchez-Vives and McCormick, 2000). In thalamic neurons, however, UP and DOWN states are more stereotypical, do not seem to involve such a great deal of synaptic activity and therefore appear to be formed more by intrinsic events (Steriade, 1993; Steriade et al., 1993c, Contreras and Steriade, 1995, Steriade et al., 1996).

An important observation *in vivo* is that the slow oscillation in thalamocortical (TC) neurons is abolished following decortication (Timofeev and Steriade, 1996). This, together with the findings that the slow oscillation in the neocortex is resistant to widespread thalamic lesions (Steriade et al., 1993b) and that similar activity is present in isolated cortical slices (Sanchez-Vives and McCormick, 2000), has led to the suggestion that the slow rhythm is predominantly a cortically-generated phenomenon. However, we have recently shown that following sustained activation of the metabotropic glutamate receptor (mGluR) that is postsynaptic to corticothalamic fibres, i.e. mGluR1a (Godwin et al., 1996; von Krosigk et al., 1999, Turner and Salt, 2000), TC neurons of the isolated cat dorsal lateral geniculate nucleus (LGN) maintained *in vitro* can exhibit an intrinsic slow oscillation (Hughes et al., 2002b, Hughes et al., 2004) which is identical to that observed during the slow rhythm in the intact brain (Steriade et al., 1993c, Contreras and Steriade, 1995, Steriade et al., 1996; Steriade, 1993). This illustrated that, at least in the LGN, TC neurons do not require rhythmic cortical input in order to generate the slow oscillation, and suggested that TC neurons might play a more active role in shaping the slow rhythm than had previously been recognised.

In this study, we further investigated the properties of the slow oscillation in LGN TC neurons and tested whether a simple 'reactivation' of modulatory cortical input *in vitro* is also able to induce equivalent activity in TC neurons from three additional thalamic relay nuclei in the cat (ventrobasal complex, VB, i.e. somatosensory thalamus; medial geniculate body, MGB, i.e. auditory thalamus; ventral lateral nucleus, VL, i.e. motor thalamus) and from two different sensory thalamic nuclei of rats and mice (LGN and VB). We find that mGluR1a-activation can bring about a stereotypical slow oscillation in TC neurons of all these additional structures with basic properties that are shared by all cells. Specifically, in each nuclei examined the slow oscillation, i) always comprised the rhythmic alternation between discrete UP and DOWN membrane potential states with the UP state being initiated by a low-threshold Ca^{2+} potential (LTCP), and ii) always increased in frequency with increasing hyperpolarization, often eventually leading to δ oscillations at ~1-4 Hz (McCormick and Pape, 1990, Leresche et al., 1991). However, outside these basic common components the slow oscillation was expressed with important differences between different nuclei. In particular, the cat LGN was found to be exceptional in that a large proportion (44%) of slow oscillations in this structure exhibit 'active' UP states comprising sustained action potential output whereas in all other cat thalamic nuclei and in the LGN and VB of both rats and mice this proportion was considerably lower. We suggest that this may reflect a rich visual nature of sleep in higher mammals and might also provide important clues for understanding the functional role of the slow oscillation in TC neurons. Some of these results have been presented in abstract form (Blethyn et al., 2002).

EXPERIMENTAL PROCEDURES

Procedures involving experimental animals were carried out in accordance with local ethical committee guidelines and the U.K. Animals (Scientific Procedure) Act, 1986. All efforts were made to minimize the suffering and number of animals used in each experiment.

Slice preparation and maintenance

Young adult cats (1-1.5 kg) were deeply anaesthetized with a mixture of O_2 and NO_2 (2:1) and 2.5% halothane, a wide craniotomy performed and the brain removed. Sagittal slices (450-500 μm) of the thalamus containing either the LGN, VB, MGB or VL were prepared and maintained as described previously (Hughes et al., 2002b, Hughes et al., 2004). Male Wistar rats (150-200g) and adult C57BL/6 mice were deeply anaesthestized (1·5 % halothane) and killed by decapitation. In both cases, coronal slices (400-450 μm) containing either the LGN or VB were prepared and maintained as in previous studies (Hughes et al., 1999). For recording, slices were perfused with a warmed (35±1 °C), continuously oxygenated (95% O_2, 5% CO_2), artificial cerebrospinal fluid (ACSF) containing (mM): NaCl (134); KCl (2); KH_2PO_4 (1.25); $MgSO_4$ (1); $CaCl_2$ (2); $NaHCO_3$ (16); glucose (10). All drugs were dissolved directly in ACSF. The following drugs were obtained from Tocris-Cookson (UK): DL-2-amino-5-phosphonovaleric acid (DL-AP5), (+)-2-methyl-4-carboxyphenylglycine (LY367385), P-(3-aminopropyl)-P-diethoxymethyl-phosphinic acid (CGP 56999A), 6-cyano-7-nitroquinoxaline-2,3-dione (CNQX), 1,2,3,4-tetrahydro-6-nitro-2,3-dioxobenzo[*f*] quinoxaline-7-sulfonamide (NBQX),. 6-imino-3-(4-methoxyphenyl)-1(6*H*)-pyridazinebutanoic acid (SR95531), (+/−)-1-aminocyclopentane-trans-1,3-dicarboxylic acid (*trans*-ACPD), tetrodotoxin (TTX). Bicuculline methiodide (BMI) was obtained from Sigma (UK).

Electrophysiology and data analysis

Extracellular recordings were performed using glass pipettes filled with 0.5 M NaCl (resistance: 1-5 MΩ) connected to a Neurolog 104 differential amplifier (Digitimer Ltd., Welwyn Garden City, UK) and bandpass filtered at 0.1-20 kHz. Intracellular recordings, using the current clamp technique, were performed with standard-wall glass microelectrodes filled with 1M potassium acetate (resistance: 80-120 MΩ), and in some cases 2% biocytin or neurobiotin, and connected to an Axoclamp-2A amplifier (Axon Instruments, Foster City, USA) operating in bridge mode. Impaled cells were identified as TC neurons using established electrophysiological and morphological criteria (Williams et al., 1996, Hughes et al., 2002a). In slices where neurons had been filled with biocytin, visualization of the dye was performed as described previously (Hughes et al., 2002a). All neurons recorded in the VB (cat, rat and mouse) were from the ventral posterior lateral nucleus (VPL) whereas all cells assessed in the MGB (cat only) were from the dorsal subdivision. A small proportion (<20%) of the cat LGN TC neurons included for analysis in this study were also included in a previous paper (Hughes et al., 2002b). Membrane potential and injected current records were stored on a Biologic DAT recorder (IntraCel, Royston, UK) and later analyzed using Clampfit (Axon Instruments). The apparent input resistance (R_N) was estimated from voltage responses evoked at −60 mV by small (20-50 pA) hyperpolarizing current steps. Statistical significance was assessed using Student's t-test. All quantitative results in the text and figures are expressed as mean±SEM.

Assessment of the different components of the slow (<1 Hz) oscillation in TC neurons with intra- and extracellular recordings

For intracellular recordings we applied 100 μM *trans*-ACPD in all cases and then varied the injected d.c. current appropriately to examine the properties of the slow (<1 Hz) oscillation, if one was present (Supp. Fig. 1A). The durations of the UP and DOWN states were taken as the time spent above and below −60 mV, respectively (Supp. Fig. 1A). In all cases, the frequency of the oscillation was taken as the reciprocal of the time between the start of successive UP states (Supp. Fig. 1A). The peak membrane potential of the UP state was computed after discarding the first 200 ms of this event. This was done to prevent a distortion of this value by the initial LTCP-mediated burst, which was always completed within this timescale. The 'active' phase of the UP state was taken as the period of firing

that occurred after the initial LTCP burst. Thus, the peak firing rate for 'active' UP states, which was computed as the reciprocal of the smallest inter-spike interval evident during the 'active' phase, also did not take into account this burst. A 'grouped' δ sequence was defined as a series of rhythmic LTCP-mediated bursts that could emerge during the slow oscillation DOWN state (Supp. Fig. 1A). To assess the properties of the slow (<1 Hz) oscillation with extracellular single unit recordings, we first induced continuous tonic firing or high-threshold (HT) bursting by applying 100-150 μM *trans*-ACPD (non-specific Group I/II mGluR agonist) (Hughes et al., 2004). This was then gradually washed off so that a slow oscillation could become apparent (Supp. Fig. 1B). In every neuron, the slow oscillation exhibited its lowest frequency at the highest concentration of *trans*-ACPD for which it was present and then progressively increased in frequency as *trans*-ACPD washed out (Supp. Fig. 1B). Upon complete washout of *trans*-ACPD, TC neurons either became quiescent or exhibited rhythmic LTCP-mediated bursting at δ frequencies (~1-4 Hz) (McCormick and Pape, 1990, Leresche et al., 1991) (Supp. Fig. 1B). This approach allowed us to examine the full behavioral repertoire and range of frequencies of the slow oscillation in each recorded cell. The majority of both extra- and intracellular recordings were performed in the presence of CNQX (or NBQX), DL-AP5, BMI (or SR95531) and CGP 56999A to block fast ionotropic glutamate, $GABA_A$ and $GABAB_B$ receptors.

RESULTS

The slow (<1 Hz) oscillation in different thalamic relay nuclei of the cat

Effects of mGluR activation assessed with intracellular recordings in the cat LGN, VB, MGB and VL—When assessed with intracellular recordings in control conditions, LGN TC neurons exhibited an apparent input resistance (R_N) of 187.0±10.1 MΩ and a resting membrane potential (V_m) of −65.0±1.1 mV (n=60). None of these neurons exhibited a slow oscillation in control conditions although 20 displayed a spontaneous δ oscillation (McCormick and Pape, 1990, Leresche et al., 1991) (Fig. $1A_1$). As described previously (Hughes et al., 2002b, 2004), application of 100 μM *trans*-ACPD expanded the oscillatory repertoire of these cells so that 60% (36 of 60) became able to generate a slow oscillation (Fig. $1A_2$). *Trans*-ACPD also caused a 142±61% increase in apparent input resistance (R_N) (Fig. 1B) and a 13±0.1 mV depolarization (n=31) (see McCormick and von Krosigk, 1992, von Krosigk et al., 1999, Turner and Salt, 2000). Expression of the slow oscillation was related to a significantly higher value of R_N (slow-oscillating neurons: 614.2±92.6 MΩ, n=34; non-oscillating neurons: 147.9±14.8 MΩ, n=19; $p<0.001$) (Table 1) and the appearance of a distinctly non-linear voltage response to small negative current steps (Fig. 1B) (Williams et al., 1997, Hughes et al., 1999, Hughes et al., 2002b).

No TC neurons in the cat VB, MGB and VL exhibited a slow oscillation in control conditions. However, 54% (14 of 26), 56% (15 of 27) and 73% (11 of 15), respectively, did so following application of 100 μM *trans*-ACPD (Figs. $2A_2$, 3 and 4). *Trans*-ACPD also led to a significant increase in R_N (VB: 195.8±30.3 to 474.6±159.5 MΩ, n=26; MGB: 216.2±25.2 to 546.3±119.8 MΩ, n=27; VL: 157.5±27.8 to 552.8±205.5 MΩ, n=15) and an appreciable membrane potential depolarization (VB: −68.5±1.7 to −56.5±1.5 mV, n=21; MGB: −64.4±0.9 to −55.3±0.7 mV, n=20; VL: −68.3±2.3 to −55.7±1.6 mV, n=13) (Fig. 2). In accordance with results in the LGN, the slow oscillation in VB, MGB and VL TC neurons was associated with a significantly larger R_N compared to non-oscillating cells ($p<0.01$ for each case, Table 1) and the appearance of a conspicuously non-linear voltage response to small hyperpolarizing current pulses (Fig. 2B). Also, as shown previously for the LGN (Hughes et al., 2002b, Hughes et al., 2004), the action of *trans*-ACPD in bringing about a slow oscillation in VB, MGB and VL TC neurons was via activation of mGluR1a since subsequent application of the mGluR1a-specific antagonist, LY367385 (300 μM),

reversibly blocked the ability of these cells to generate this activity (n=5) (Figs. $2A_3$) (see also Turner and Salt, 2000).

In all types of cat TC neurons, the slow oscillation was extremely robust and could often remained unaltered and uninterrupted for long recording periods (up to 6 hours). No clear morphological differences were detected between oscillating and non-oscillating neurons in the LGN, VB, MGB or VL.

Essential common properties of the slow (<1 Hz) oscillation—In all cat thalamic relay nuclei examined, the slow oscillation shared a number of basic common properties (Fig. 3). These included, i) the stereotypical alternation between UP and DOWN membrane potential states that were separated by ~20 mV, ii) the commencement of each UP state with an LTCP-mediated burst (Fig. $3A_1$), iii) a transition from the UP to DOWN state that was marked by a clear membrane potential inflection (Fig. $3A_1$), and iv) a hyperpolarization-activated mixed cation current (I_h)-dependent slow depolarization during the DOWN state (Fig. $3A_1$) (Hughes et al., 2002b). Also common to all types of cat TC neurons was the finding that hyperpolarization (achieved through injecting negative d.c. current) always increased the frequency of the slow oscillation until it was often eventually transformed into a continuous δ oscillation (Fig. 3; see also Figs. 1, 2, 6, 7 and 8). This increase in frequency overwhelmingly resulted from a shortening of the UP state (LGN: from 11.3±2.4 to 1.4±0.2 s, n=26 neurons; VB: from 14.1±5.6 to 1.5±0.4 s, n=8 neurons; MGB: from 17.1±3.7 to 2.3±0.6 s, n=7 neurons; VL: from 48.5±14.2 to 3.9±1.3 s, n=6 neurons; $p<0.05$ for each nucleus) with the duration of the DOWN state remaining essentially unchanged (LGN range: 1.0±0.2 to 1.4±0.2 s, n=26 neurons; VB range: 1.0±0.2 to 1.2±0.2 s, n=8 neurons; MGB range: 0.9±0.1 to 1.4±0.2 s, n=7 neurons; VL range: 1.2±0.2 to 1.3±0.3 s, n=6 neurons; $p>0.1$ for each nucleus) (Fig 3; ee also Fig. $6A_3$ and $6B_3$ and Table 1). The mean minimum frequencies of the slow oscillation recorded intracellularly in LGN, VB, MGB and VL TC neurons were 0.3±0.04 Hz (n=34), 0.12±0.04 Hz (n=11), 0.06±0.03 Hz (n=14) and 0.04±0.02 Hz (n=8) respectively.

Nucleus-specific properties of the slow (<1 Hz) oscillation in the cat thalamus

Prevalence of different manifestations of the slow (<1 Hz) oscillation in LGN, VB, MGB and VL TC neurons—Slow oscillations observed with intracellular recordings in the LGN occurred with a remarkably large variety of manifestations. Most neurons displayed an oscillation possessing an UP state that was always ‘quiescent’, i.e. that did not exhibit further firing, following the initial LTCP burst (‘quiescent’ slow oscillation) (24 of 36; 67%) (Figs. 4A, 4B, 6A and 8A). However, in the remainder of cells (12 of 36; 33%), the UP state could be characterised by the sustained firing of either single action potentials (i.e. tonic firing) (n=6) (Figs. $4C_1$ and $4D_1$), a mixture of single action potentials and high-threshold (HT) bursts (see Hughes et al. 2002b, 2004) (n=3) (Figs. $4C_2$ and 7A) or HT bursts only (n=3) (Figs. $4C_3$) (‘active’ slow oscillation). Both the ‘quiescent’ (Fig. 4B) and ‘active’ (Fig. 4D) forms of the slow oscillation could exhibit ‘grouping’ of the δ oscillation (21%, n=5 of 24, and 33%, n=4 of 12, respectively) (Steriade et al., 1993c; Hughes et al., 2002b) whereby the DOWN state could be replaced by transient sequences of rhythmic LTCP-mediated bursts at ~1-4 Hz (‘grouped’ δ sequences) (Figs. 4B, 4D and 8A).

In contrast to the cat LGN, the expression of the slow oscillation in the cat VB, MGB and VL was considerably less heterogeneous (Figs. 3B-D and 5). The vast majority of intracellularly recorded VB TC neurons exhibited slow oscillations that were of the ‘quiescent’ type (93%; 13 of 14) (Figs. 3B and 5A) with only one neuron able to generate an ‘active’ slow oscillation (comprising tonic firing only, see below and Fig. 7B). For the VB, ‘grouped’ δ sequences were only apparent in 4 neurons that displayed ‘quiescent’ slow

oscillations (Fig. $5A_2$). Intracellularly recorded slow oscillations in MGB and VL TC neurons were always of the 'quiescent' type (Figs. 3C, 3D, 5B, 5C, 6B and 8B) with δ 'grouping' being present in 8 (of 15) and 2 (of 11) cells, respectively (Figs. $5B_2$, $5C_2$, 8B).

Specific properties of different manifestations of the slow oscillation in cat thalamic nuclei—In LGN TC neurons displaying a 'quiescent' slow oscillation, the peak membrane potential reached during the UP state increased with depolarization (Fig. 6A). Interestingly, at its maximum (−48.3±0.7 mV; n=23) this value could exceed some of the stable membrane potentials reached by the same neurons when they were subjected to more steady depolarizing current (Fig. $6A_1$ and $6A_2$) and, specifically, was significantly larger than the average resting membrane potentials of those cells that displayed a stable membrane potential in the absence of steady current (i.e. rather than a slow oscillation) ($p<0.01$) (Fig. and Table 1; see also Fig. 3). The peak membrane potentials reached during the UP state of 'quiescent' slow oscillations in VB, MGB and VL neurons also increased as neurons were depolarized and at their maximums were −56.1±1.8 mV (n=11), −54.7±1.4 mV (n=14) and −53.3±1.6 mV (n=8), respectively (Fig. 6B and Table 1). Again, these values could be greater than some of the stable membrane potentials exhibited by the same neurons in response to additional steady depolarizing current (Fig. $6B_1$ and $6B_2$), were comparable with the average resting membrane potentials of those cells that displayed a steady membrane potential in the absence of d.c. current ($p>0.1$) (Table 1; see also Fig. 3), but were all significantly lower than the equivalent value for LGN TC neurons ($p<0.01$ for each case).

For 'active' slow oscillations, an increase in the 'excitability' level of the UP state also occurred with depolarization with this being reflected as a progressive increase in both the frequency and the extent of firing (Fig. 7). In fact, the peak firing frequency during the UP state commonly reached values that were comparable with or greater than those observed in neurons displaying continuous, spontaneous action potential output in the absence of any steady d.c. current (i.e. when neurons are subject to less steady hyperpolarizing d.c. current than during the slow oscillation) (LGN: maximum peak frequency of tonic firing during UP state: 11.6±3.4 Hz; spontaneous tonic firing at 0 pA d.c. current: 10.2±1.2 Hz, n=7; p=0.61. maximum inter-burst frequency of HT bursting during UP state: 6.5±1.2 Hz; spontaneous HT bursting at 0 pA d.c. current: 6.7±1.1 Hz, n=3; p=0.91) (Fig. 7A and Table 1) (VB: maximum peak frequency of tonic firing during UP state: 23.6 Hz, spontaneous tonic firing at 0 pA d.c current: 12.6 Hz) (Fig. 7B and Table 1).

In all types of cat TC neurons exhibiting 'grouped' δ activity, this 'grouping' occurred as a transition stage between a 'pure' slow oscillation and continuous δ (~1-4 Hz) activity (Fig. 8B). Thus, the overall increase in slow oscillation frequency that occurred as these cells were hyperpolarized was also affected by the dynamics of the 'grouped' δ sequences. Specifically, the number of LTCP bursts per sequence, and consequently the sequence duration (Fig. $8A_2$ and $8B_2$), increased as neurons were hyperpolarized whereas the inter-burst frequency remained constant (Fig. $8A_3$ and $8B_3$). 'Grouped' δ sequences were generally least extensive (i.e. of shortest duration) in the LGN (LGN: max. bursts per sequence: 5.5±1.1; mean inter-burst frequency: 1.7±0.2 Hz, n=9; VB: max. bursts per sequence: 7.2±1.0; mean inter-burst frequency: 1.6±0.1 Hz, n=4; MGB: max. bursts per sequence: 10.8±5.3; mean inter-burst frequency: 1.2±0.1 Hz, n=7; VL: max. bursts per sequence: 15.4±3.2; mean inter-burst frequency: 1.4±0.1 Hz, n=2) (Table 1).

Extracellular recordings of the slow (<1 Hz) oscillation in cat thalamic nuclei—The essential pattern of findings obtained with intracellular recordings in different cat thalamic nuclei was also evident with extracellular single unit recordings (see Supp. Information and Supp. Table 1). In particular, the most widespread array of slow oscillations

was clearly observed in the LGN (Fig. 11 and Supp. Fig. 2) whereas 'grouped' δ sequences were more extensive (i.e. of longer duration) in other nuclei (Supp. Fig. 3 and Supp. Table 1). However, one clear difference between intra- and extracellular recordings was that during the latter, we encountered a larger number of neurons that exhibited 'active' slow oscillations (Fig. 11 and Supp. Fig. 3). Indeed, whereas during intracellular recordings we did not observe any 'active' slow oscillations in the cat MGB or VL and only one in the VB, during extracellular recordings, 19% (8 of 43), 14% (6 of 42) and 14% (4 of 28) of VB, MGB and VL neurons, respectively, showed an 'active' oscillation. In addition, in the VB, one of these 'active' oscillations involved HT bursts, a phenomenon that was not observed with intracellular recordings (n=1 of 8) (Supp. Fig. $3A_3$). For the LGN, an 'active' slow oscillation was present in 56% (19 of 34) of extracellular recordings. Thus, when intra- and extracellular recordings were considered together, 'active' slow oscillations accounted for 44% 16%, 11% and 10% of cases in the LGN, VB, MGB and VL, respectively. A full description of the results obtained with extracellular recordings in different cat thalamic nuclei is given in the supplementary information and in Supplementary Table 1 and Fig. 11.

LGN and VB of the rat and mouse

Intracellular recordings of the slow oscillation in the rat LGN—Rat LGN TC neurons examined with intracellular recordings in control exhibited an R_N of 198.0±18.0 MΩ and a V_m of −64.8±0.9 mV (n=10) (Fig. 9A). None of these cells displayed a slow oscillation in control conditions. However, application of 100 μM *trans*-ACPD brought about a slow oscillation (with basic components that were equivalent to those observed in cat thalamic nuclei, see above) in 40% (4 of 10) of cases (Fig $9B_1$ and Supp. Fig. 4A). Intracellularly recorded slow oscillations in rat TC neurons were always of the 'quiescent' type. The presence of the slow oscillation was linked with a larger value of R_N (slow-oscillating neurons: 1040.0±272.6 MΩ, n=4; non-oscillating neurons: 325.2±68.0 MΩ, n=6; $p<0.01$) and the advent of an overtly non-linear voltage response to the challenge of small negative current steps (Fig. $9A_2$). Also in direct correspondence with cat TC neurons, the frequency of the slow oscillation in the rat increased with hyperpolarization until a continuous δ oscillation became apparent (Fig $9B_1$ and $9B_3$). The mean minimum frequency of the slow oscillation recorded intracellularly in rat LGN TC neurons was 0.25±0.05 Hz (n=4). The peak membrane potential of the UP state of the slow oscillation in the rat increased as neurons were depolarized and at its maximum was −57.6±0.8 mV (n=4) (Fig. $9B_2$). This value was comparable with the resting membrane potential of these cells (−57.4±0.7 mV; n=4; p=0.89) but was less than the equivalent values obtained from all types of cat TC neurons (see above and Table 1).

Extracellular recordings in the rat LGN and VB—Slow oscillations were also clearly evident in extracellular single unit recordings from the rat LGN and VB (Fig. 9C and Supp. Fig. 4B). Interestingly, as in the cat, these recordings revealed the presence of a small proportion of 'active' slow oscillations so that 14% (2 of 14) and 10% (1 of 10) of slow oscillations observed with extracellular recordings in the LGN and VB, respectively, were of this type (Fig. $9C_1$ and Supp. Fig. $4B_2$). Furthermore, in one of the LGN TC neurons, the 'active' oscillation involved HT bursts (Fig. $9C_1$), a phenomenon which was not evident with intracellular recordings. When intra- and extracellular recordings were considered together, 'active' slow oscillations accounted for 8% of cases in the rat LGN. A more detailed description of the results obtained with extracellular recordings in the rat LGN and VB is given in the Supplementary Information and Supplementary Table 1.

Intra- and extracellular recordings in the mouse LGN and VB—In control conditions, intracellularly recorded TC neurons in the mouse LGN and VB exhibited an R_N of 140.2±22.5 MΩ and a V_m of −60.2±1.2 mV (n=10). None of these neurons exhibited a

slow oscillation in control conditions. Application of *trans*-ACPD (100 μM) led to a small change in V_m (3.5±0.8 mV; n=10) and increase in R_N (44.2±12.1%; n=10) but did not bring about a slow oscillation in any cells (Fig. 10A). In addition, *trans*-ACPD application was not associated with the appearance of a non-linear charging pattern in response to small negative current steps in any mouse TC neuron (Fig. $10A_2$).

The slow oscillation *is* present in mouse TC neurons, however, because extracellular single unit recordings obtained from the mouse LGN and VB were characterised by this activity in 78% (28 of 36) and 27% (12 of 44) of cases respectively (Figs. 10B and 10C and Supp. Fig. 5). For LGN recordings, 89% (25 of 28) of slow oscillations were 'quiescent' whilst 11% (3 of 28; 1 involving HT bursts) were 'active' (Figs. 10B and 10C). The equivalent values for the mouse VB were 92% (11 of 12) and 8% (1 of 12), respectively. 'Active' firing in mouse TC neurons exhibited properties that were essentially equivalent to those observed in cat and rat TC neurons (Fig. 10C and Supp. Information and Supp. Table 1). We observed δ 'grouping' in one 'quiescent' slow oscillation in the mouse VB (Supp. Fig. 5A). Further details regarding the properties and prevalence of the slow oscillation in different rat and mouse thalamic nuclei are given in Table 1, Supplementary Table 1 and Fig. 11.

DISCUSSION

The main findings of this study are, i) the stereotypical slow (<1 Hz) oscillation is present in TC neurons of the cat LGN, VB, MGB and VL, and of the rat and mouse LGN and VB; ii) in all cases, the slow oscillation increases in frequency as the depolarizing drive to TC neurons is reduced (either through the injection of hyperpolarizing d.c. current or a decrease in the intensity of mGluR1a-activation); iii) this increase in frequency overwhelmingly occurs through a shortening of the UP state; iv) in 44% of cases, the UP state of the slow oscillation in LGN TC neurons is characterised by the sustained firing of either single action potentials and/or HT bursts ('active' slow oscillation). This occurs considerably less often for slow oscillations in other thalamic nuclei of the cat and in each nucleus examined in the rat and mouse; and v) the peak membrane potential reached (for 'quiescent' oscillations) or the peak rate of firing observed (for 'active' oscillations) during the UP state can exceed levels exhibited when neurons are depolarized above the range where slow oscillations occur, with this being most pronounced in the LGN.

The slow (<1 Hz) oscillation as a common property of TC neurons with shared fundamental properties

Although we observed a variety of manifestations of the slow oscillation during this study a number of fundamental elements were shared by all neurons regardless of species or nuclei. First, in all neurons the slow oscillation was expressed as the rhythmic alternation between UP and DOWN membrane potential states. Second, the slow oscillation UP state always started with an LTCP-mediated burst. Third, the UP state was always terminated by a marked, stereotypical inflection point before transition to the DOWN state. Fourth, during the DOWN state, an overt slow depolarization (due to the mixed cation current, I_h; McCormick and Pape, 1990, Soltesz et al., 1991) was always evident before the reappearance of the UP state and the repetition of the oscillation cycle. Importantly, and as discussed previously (Hughes et al., 2002b), these common slow oscillation components are clearly evident during slow oscillations observed in TC neurons *in vivo* (Steriade, 1993; Steriade et al., 1993c, Contreras and Steriade, 1995, Steriade et al., 1996).

Perhaps one of the most striking observations in this study was that for any given level of injected d.c. current these basic elements of the slow oscillation were both extremely robust (i.e. they could remain unaltered and uninterrupted for several hours) and remarkably well conserved from cycle to cycle. We suggest that this combination of robustness and

reproducibility renders the slow oscillation (<1 Hz) ideally suited as a reliable pacemaker of rhythmic cortical activity. Thus, although it is well established that the cortex can generate a slow oscillation in the absence of thalamic input (Steriade et al., 1993b; see also Sanchez-Vives and McCormick, 2000), and whilst we therefore do not claim that the thalamus is solely responsible for generating the slow (<1 Hz) rhythm in the intact brain, this study lends further support to the argument that the TC neuron slow oscillation, at the very least, plays an active role in shaping the overall slow rhythm. The precise way in which the cortex and thalamus interact in this manner, however, remains to be fully understood.

Nucleus- and species-specific differences and their functional significance

We observed a number of important nucleus- and species-specific differences in the slow oscillation. The most prominent distinction was that when extra- and intracellular recordings were considered together, 44% of cat LGN TC neurons exhibited a slow oscillation which could display ‘active’ UP states whereas the proportion of ‘active’ slow oscillations present in all other types of TC neurons was at most 16% (see Fig. 11). Furthermore, outside the LGN, an ‘active’ slow oscillation was only evident with intracellular recordings in one cat VB TC neuron. Since it is well known that in comparison to other cat thalamic nuclei the LGN contains TC neurons that show a diverse range of morphologies and soma sizes (Friedlander et al., 1979), it is a distinct possibility that differences in the expression of the slow oscillation are related to the morphological complexity and heterogeneity of cells in this structure. Unfortunately, we did not collect sufficient morphological data in this study to definitively address this issue. However, our preliminary data suggests that ‘active’ slow oscillations may be associated with a smaller soma size (see Fig. 4) which is clearly consistent with the general finding that ‘active’ oscillations are more prevalent in extracellular recordings compared to intracellular recordings (see Fig. 11).

Other possible reasons for the preponderance of ‘active’ UP states in LGN TC neurons might be related to the expression of the ionic currents that shape the slow oscillation. We have previously shown that the slow oscillation in TC neurons arises when mGluR activation sufficiently reduces the leak K^+ current, I_{Leak}, below a threshold where it can then interact with the ‘window’ component of the T-type Ca^{2+} current, $I_{Twindow}$, to produce a form of intrinsic membrane potential bistability (Williams et al., 1997; Tóth et al., 1998; Hughes et al., 2002b). In simplified terms, this bistability dictates that the slow oscillation UP state corresponds to $I_{Twindow}$ being ‘switched on’ whereas the DOWN state is related to it being ’switched off’’ (see Figs. 1 and 4 in Crunelli et al., 2005). The UP state is also profoundly enhanced by a Ca^{2+}-activated non-selective current (I_{CAN}) (for a detailed explanation of the ionic mechanisms underlying the slow oscillation see Crunelli et al., 2005 and Crunelli et al., 2006). Thus, we expect that the balance between the inward currents that contribute to the UP state (i.e. $I_{Twindow}$ and I_{CAN}) and the outwardly rectifying K^+ channels that are present in TC neurons (Huguenard et al., 1991, Huguenard and Prince, 1991, Turner et al., 1997) is especially crucial in determining the precise manifestation of the slow oscillation. As such, LGN neurons which exhibit ‘active’ UP states might possess either an especially large I_{CAN} and/or I_T, or express smaller outwardly rectifying K^+ currents. Interestingly, it has been previously shown that TC neurons in the cat VB exhibit particularly strong outward rectification (Turner et al., 1997) compared to LGN TC neurons (Pirchio et al., 1997), which is coherent with the lower membrane potential reached during the UP state in these cells compared to those in the LGN and, therefore, the predominance of ‘quiescent’ slow oscillations in the VB.

When considered at the functional level, the large percentage of TC neurons in the cat LGN that exhibit ‘active’ slow oscillations is clearly consistent with the idea that during sleep, the visual systems of higher mammals exhibit an elevated level of activity compared to other modalities (see Symons, 1993). However, regardless of the precise manifestation of the slow

Europe PMC Funders Author Manuscripts

oscillation, the UP state generally represents a substantially excited state since it exhibits either a peak membrane potential or firing rate not normally observed unless neurons are depolarized above the range where the slow oscillation occurs. This suggests that even 'quiescent' UP states in TC neurons are highly conducive to information processing (see Steriade, 2001, Steriade et al., 2001). In connection with this, we suggest that the presence of an LTCP-mediated burst at the commencement of each UP state may be a mechanism whereby the thalamus is sending a specific priming signal to the cortex that the 'activated' or 'processing' phase of the slow oscillation is about to begin (Steriade, 2001, Steriade et al., 2001). Of course, the idea that the LTCP-mediated bursts of the slow oscillation signal the upcoming transmission of high-priority information is essentially equivalent to that which has been suggested for the role of LTCP-mediated bursts in TC neurons during wakefulness (Sherman, 2001a, Sherman, 2001b). Indeed, we have recently postulated that similar cellular mechanisms may underlie both the slow oscillation and the ability to generate LTCP-mediated bursts from depolarized membrane potentials during the wake state (Crunelli et al., 2005).

Supplementary Material

Refer to Web version on PubMed Central for supplementary material.

Acknowledgments

We wish to thank Mr. T.M. Gould for technical assistance. This work was supported by the Wellcome Trust (grant 71436). Additional information regarding this and other published work from the Crunelli lab is available at http://www.thalamus.org.uk.

ABBREVIATIONS

ACSF	Artificial cerebrospinal fluid
BMI	Bicuculline methiodide
CGP 56999A	P-(3-aminopropyl)-P-diethoxymethyl-phosphinic acid
CNQX	6-cyano-7-nitroquinoxaline-2,3-dione
DL-AP5	DL-2-amino-5-phosphonovaleric acid
EEG	Electroencephalogram
HT	High-threshold
$\mathbf{I_{CAN}}$	Ca^{2+}-activated non-selective cation current
$\mathbf{I_h}$	Hyperpolarization-activated mixed cation current
$\mathbf{I_{Leak}}$	Leak K^+ current
$\mathbf{I_T}$	T-type Ca^{2+} current
$\mathbf{I_{Twindow}}$	T-type Ca^{2+} 'window' current
LGN	Dorsal lateral geniculate nucleus
LTCP	Low-threshold calcium potential
LY367385	(+)-2-methyl-4-carboxyphenylglycine
MGB	Medial geniculate body
mGluR	Metabotropic glutamate receptor

NBQX	1,2,3,4-tetrahydro-6-nitro-2,3-dioxobenzo[*f*]quinoxaline-7-sulfonamide
NREM	Non-rapid eye movement
R_N	Apparent input resistance
SR95531	6-imino-3-(4-methoxyphenyl)-1(6*H*)-pyridazinebutanoic acid
TC	Thalamocortical
***trans*-ACPD**	(+/−)-1-aminocyclopentane-trans-1,3-dicarboxylic acid
TTX	Tetrodotoxin
VB	Ventrobasal complex
VPL	Ventral posterior lateral nucleus
VL	Ventral lateral nucleus
V_m	Resting membrane potential

REFERENCES

Achermann P, Borbely AA. Low-frequency (< 1 Hz) oscillations in the human sleep electroencephalogram. Neuroscience. 1997; 81:213–222. [PubMed: 9300413]

Amzica F, Steriade M. The K-complex: its slow (<1-Hz) rhythmicity and relation to delta waves. Neurology. 1997; 49:952–959. [PubMed: 9339673]

Amzica F, Steriade M. Cellular substrates and laminar profile of sleep K-complex. Neuroscience. 1998; 82:671–686. [PubMed: 9483527]

Blethyn KL, Hughes SW, Cope DW, Crunelli V. Nucleus-specific properties of the slow (<1 Hz) oscillation in thalamic neurones in vitro. Society for Neuroscience Abstracts. 2002; 28:352.4.

Contreras D, Steriade M. Cellular basis of EEG slow rhythms: a study of dynamic corticothalamic relationships. J Neurosci. 1995; 15:604–622. [PubMed: 7823167]

Crunelli V, Cope DW, Hughes SW. Thalamic T-type calcium channels and NREM sleep. Cell Calcium. 2006 In Press.

Crunelli V, Toth TI, Cope DW, Blethyn K, Hughes SW. The 'window' T-type calcium current in brain dynamics of different behavioural states. J Physiol. 2005; 562:121–129. [PubMed: 15498803]

Domich L, Oakson G, Steriade M. Thalamic burst patterns in the naturally sleeping cat: a comparison between cortically projecting and reticularis neurones. J Physiol (Lond). 1986; 379:429–449. [PubMed: 3560000]

Friedlander MJ, Lin CS, Sherman SM. Structure of physiologically identified X and Y cells in the cat's lateral geniculate nucleus. Science. 1979; 204:1114–1117. [PubMed: 451559]

Godwin DW, Van Horn SC, Eriir A, Sesma M, Romano C, Sherman SM. Ultrastructural localization suggests that retinal and cortical inputs access different metabotropic glutamate receptors in the lateral geniculate nucleus. J Neurosci. 1996; 16:8181–92. [PubMed: 8987843]

Hughes SW, Blethyn KL, Cope DW, Crunelli V. Properties and origin of spikelets in thalamocortical neurones in vitro. Neuroscience. 2002a; 110:395–401. [PubMed: 11906781]

Hughes SW, Cope DW, Blethyn KL, Crunelli V. Cellular mechanisms of the slow (<1 Hz) oscillation in thalamocortical neurons in vitro. Neuron. 2002b; 33:947–958. [PubMed: 11906700]

Hughes SW, Cope DW, Tóth TI, Williams SR, Crunelli V. All thalamocortical neurones possess a T-type Ca^{2+} 'window' current that enables the expression of bistability-mediated activities. J Physiol. 1999; 517:805–815. [PubMed: 10358120]

Hughes SW, Lorincz M, Cope DW, Blethyn KL, Kekesi KA, Parri HR, Juhasz G, Crunelli V. Synchronized oscillations at alpha and theta frequencies in the lateral geniculate nucleus. Neuron. 2004; 42:253–268. [PubMed: 15091341]

Huguenard JR, Coulter DA, Prince DA. A fast transient potassium current in thalamic relay neurons: kinetics of activation and inactivation. J Neurophysiol. 1991; 66:1304–1315. [PubMed: 1662262]

Huguenard JR, Prince DA. Slow inactivation of a TEA-sensitive K current in acutely isolated rat thalamic relay neurons. J Neurophysiol. 1991; 66:1316–1328. [PubMed: 1761985]

Lee J, Kim D, Shin HS. Lack of delta waves and sleep disturbances during non-rapid eye movement sleep in mice lacking alpha1G-subunit of T-type calcium channels. Proc Natl Acad Sci U S A. 2004; 101:18195–18199. [PubMed: 15601764]

Leresche N, Lightowler S, Soltesz I, Jassik-Gerschenfeld D, Crunelli V. Low-frequency oscillatory activities intrinsic to rat and cat thalamocortical cells. J Physiol (Lond). 1991; 441:155–174. [PubMed: 1840071]

McCormick DA, Pape HC. Properties of a hyperpolarization-activated cation current and its role in rhythmic oscillation in thalamic relay neurones. J Physiol (Lond). 1990; 431:291–318. [PubMed: 1712843]

McCormick DA, von Krosigk M. Corticothalamic activation modulates thalamic firing through glutamate “metabotropic” receptors. Proc Natl Acad Sci U S A. 1992; 89:2774–2778. [PubMed: 1313567]

Pinault D, Vergnes M, Marescaux C. Medium-voltage 5-9 Hz oscillations give rise to spike-and-wave discharges in a genetic model of absence epilepsy: in vivo dual extracellular recording of thalamic relay and reticular neurons. Neuroscience. 2001; 105:181–201. [PubMed: 11483311]

Pirchio M, Turner JP, Williams SR, Asprodini E, Crunelli V. Postnatal development of membrane properties and delta oscillations in thalamocortical neurons of the cat dorsal lateral geniculate nucleus. J Neurosci. 1997; 17:5428–5444. [PubMed: 9204926]

Sanchez-Vives MV, McCormick DA. Cellular and network mechanisms of rhythmic recurrent activity in neocortex. Nat Neurosci. 2000; 3:1027–1034. [PubMed: 11017176]

Sherman SM. Tonic and burst firing: dual modes of thalamocortical relay. Trends Neurosci. 2001a; 24:122–126. [PubMed: 11164943]

Sherman SM. A wake-up call from the thalamus. Nat Neurosci. 2001b; 4:344–346. [PubMed: 11276218]

Soltesz I, Lightowler S, Leresche N, Jassik-Gerschenfeld D, Pollard CE, Crunelli V. Two inward currents and the transformation of low-frequency oscillations of rat and cat thalamocortical cells. J Physiol (Lond). 1991; 441:175–197. [PubMed: 1667794]

Steriade, M. Cellular substrates of bran rhythms. In: Lopes da Silva, FH., editor. Electroencephalography: Basic Principles, clinical applications, and related fields. Williams and Wilkins; Baltimore: 1993. p. 97-117.

Steriade M, Nunez A, Amzica F. A novel slow (< 1 Hz) oscillation of neocortical neurons in vivo: depolarizing and hyperpolarizing components. J Neurosci. 1993a; 13:3252–3265. [PubMed: 8340806]

Steriade M, Nunez A, Amzica F. Intracellular analysis of relations between the slow (< 1 Hz) neocortical oscillation and other sleep rhythms of the electroencephalogram. J Neurosci. 1993b; 13:3266–3283. [PubMed: 8340807]

Steriade M, Contreras D, Dossi R. Curro, Nunez A. The slow (< 1 Hz) oscillation in reticular thalamic and thalamocortical neurons: scenario of sleep rhythm generation in interacting thalamic and neocortical networks. J Neurosci. 1993c; 13:3284–3299. [PubMed: 8340808]

Steriade M, Amzica F, Contreras D. Synchronization of fast (30-40 Hz) spontaneous cortical rhythms during brain activation. J Neurosci. 1996; 16:392–417. [PubMed: 8613806]

Steriade M. Active neocortical processes during quiescent sleep. Arch Ital Biol. 2001; 139:37–51. [PubMed: 11256186]

Steriade M, Timofeev I, Grenier F. Natural waking and sleep states: a view from inside neocortical neurons. J Neurophysiol. 2001; 85:1969–1985. [PubMed: 11353014]

Symons D. The stuff that dreams aren’t made of: why wake-state and dream-state sensory experiences differ. Cognition. 1993; 47:181–217. [PubMed: 8370242]

Timofeev I, Grenier F, Steriade M. Disfacilitation and active inhibition in the neocortex during the natural sleep-wake cycle: an intracellular study. Proc Natl Acad Sci U S A. 2001; 98:1924–1929. [PubMed: 11172052]

Timofeev I, Steriade M. Low-frequency rhythms in the thalamus of intact-cortex and decorticated cats. J Neurophysiol. 1996; 76:4152–4168. [PubMed: 8985908]

Tóth TI, Hughes SW, Crunelli V. Analysis and biophysical interpretation of bistable behaviour in thalamocortical neurons. Neuroscience. 1998; 87:519–523. [PubMed: 9740410]

Turner JP, Anderson CM, Williams SR, Crunelli V. Morphology and membrane properties of neurones in the cat ventrobasal thalamus in vitro. J Physiol (Lond). 1997; 505:707–726. [PubMed: 9457647]

Turner JP, Salt TE. Synaptic activation of the group I metabotropic glutamate receptor mGlu1 on the thalamocortical neurons of the rat dorsal lateral geniculate nucleus in vitro. Neuroscience. 2000; 100:493–505. [PubMed: 11098112]

von Krosigk M, Monckton JE, Reiner PB, McCormick DA. Dynamic properties of corticothalamic excitatory postsynaptic potentials and thalamic reticular inhibitory postsynaptic potentials in thalamocortical neurons of the guinea-pig dorsal lateral geniculate nucleus. Neuroscience. 1999; 91:7–20. [PubMed: 10336055]

Williams SR, Tóth TI, Turner JP, Hughes SW, Crunelli V. The 'window' component of the low threshold Ca^{2+} current produces input signal amplification and bistability in cat and rat thalamocortical neurones. J Physiol. 1997; 505:689–705. [PubMed: 9457646]

Williams SR, Turner JP, Anderson CM, Crunelli V. Electrophysiological and morphological properties of interneurones in the rat dorsal lateral geniculate nucleus in vitro. J Physiol (Lond). 1996; 490:129–147. [PubMed: 8745283]

Europe PMC Funders Author Manuscripts

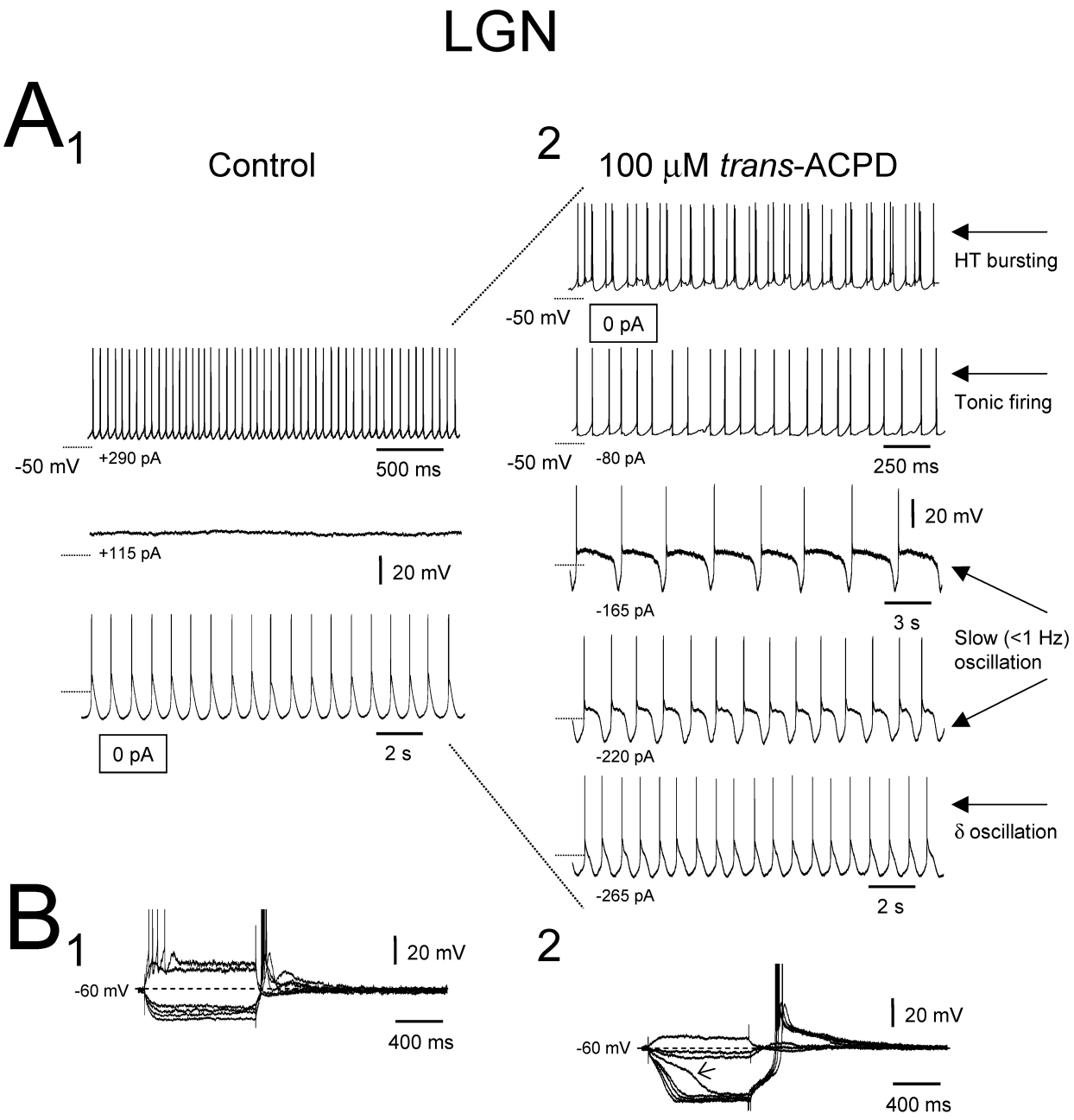

Figure 1. Effect of *trans*-ACPD on the oscillatory properties of TC neurons in the cat LGN

A_1. Intracellular recording of a cat LGN TC neuron in control conditions showing different types of activity depending on the level of injected d.c. current. In the absence of injected d.c. current the neuron displays rhythmic LTCP-mediated bursts at ~1 Hz (i.e. δ oscillation, bottom trace). When the neuron is depolarized it initially becomes silent (middle trace) and then exhibits tonic firing (top trace). **A_2**. 100 μM *trans*-ACPD expands the oscillatory repertoire of the neuron so that it includes a slow oscillation (3rd and 4th traces from the top) and HT bursting (top trace). Note that the neuron is now depolarized so that HT bursting becomes the spontaneous activity in the absence of injected d.c. current. Unless otherwise stated all dotted lines in **A_1** and **A_2** indicate −60 mV. **B**. Voltage response of the

neuron depicted in **A** to a range of injected current steps before (**1**) and after (**2**) *trans*-ACPD application. Note the appearance of a distinctly non-linear membrane charging pattern in $\mathbf{B_2}$ which encompasses a marked inflection point (↙). In this and subsequent figures some action potentials have been truncated for clarity.

Europe PMC Funders Author Manuscripts

Europe PMC Funders Author Manuscripts

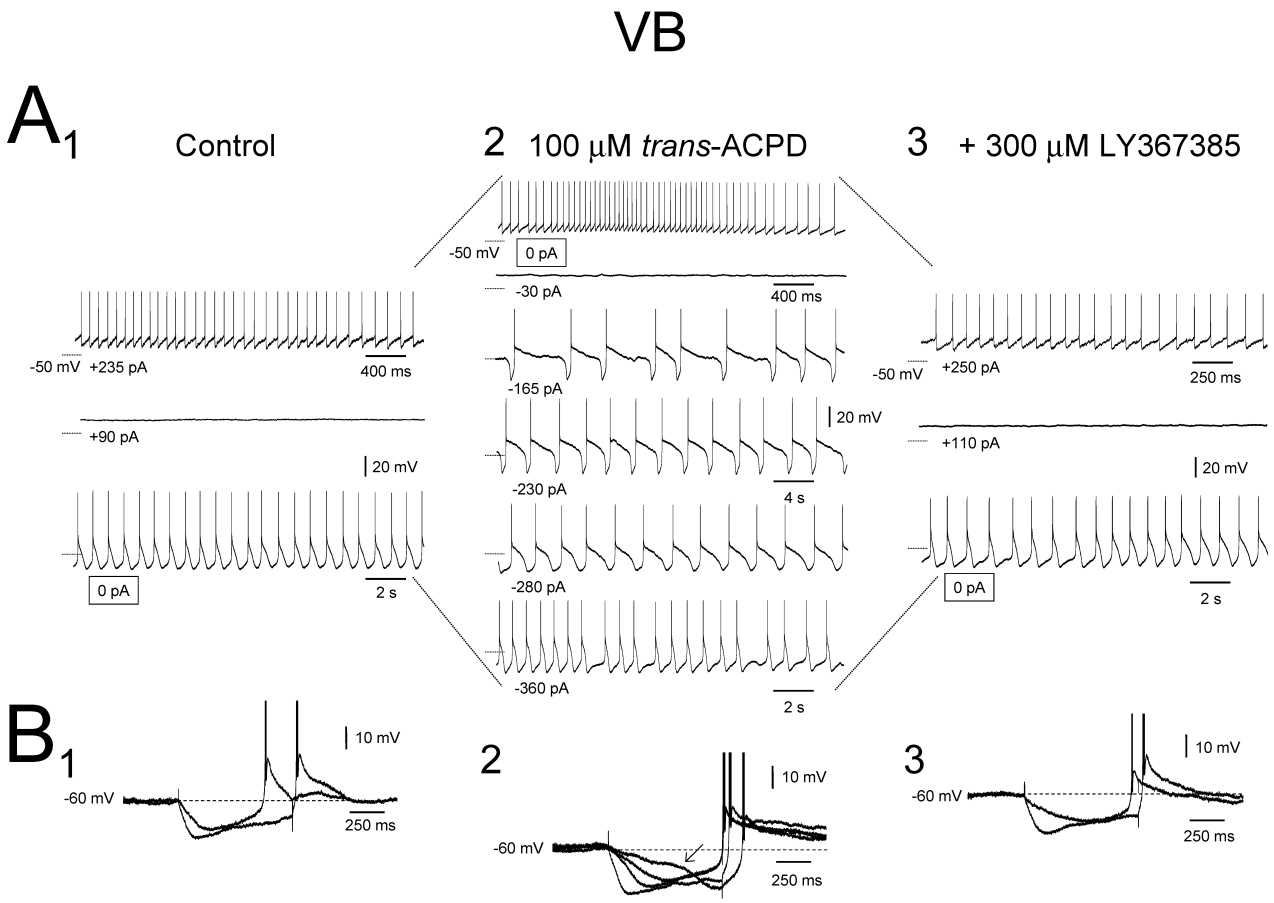

Figure 2. Effect of mGluR1a-activation in TC neurons of the cat VB

A_1. Intracellular recording of a cat VB TC neuron in control conditions showing different types of activity depending on the level of injected d.c. current. The spontaneous activity of this neuron comprises rhythmic LTCP-mediated bursts at ~1 Hz (i.e. δ oscillation, bottom trace). When the neuron is depolarized it initially becomes silent (middle trace) and then exhibits tonic firing (top trace). **A_2**. 100 µM *trans*-ACPD expands the oscillatory repertoire of the neuron so that it includes a slow oscillation (3rd, 4th, and 5th traces from the top). Note that the neuron is now depolarized so that tonic firing becomes the spontaneous activity (top trace). **A_3**. Antagonism of mGluR1a with 300 µM LY367385 returns the neuron to the control scenario. Unless otherwise stated all dotted lines in **A_1**, **A_2** and **A_3** indicate −60 mV. **B**. Voltage response of the neuron depicted in **A** to a range of injected current steps before (**1**) and after (**2**) *trans*-ACPD application, and in the subsequent presence of LY367385 (**3**). Note the appearance of a distinctly non-linear membrane charging pattern in **B_2** which encompasses a marked inflection point (↙) and its elimination following LY367385 application.

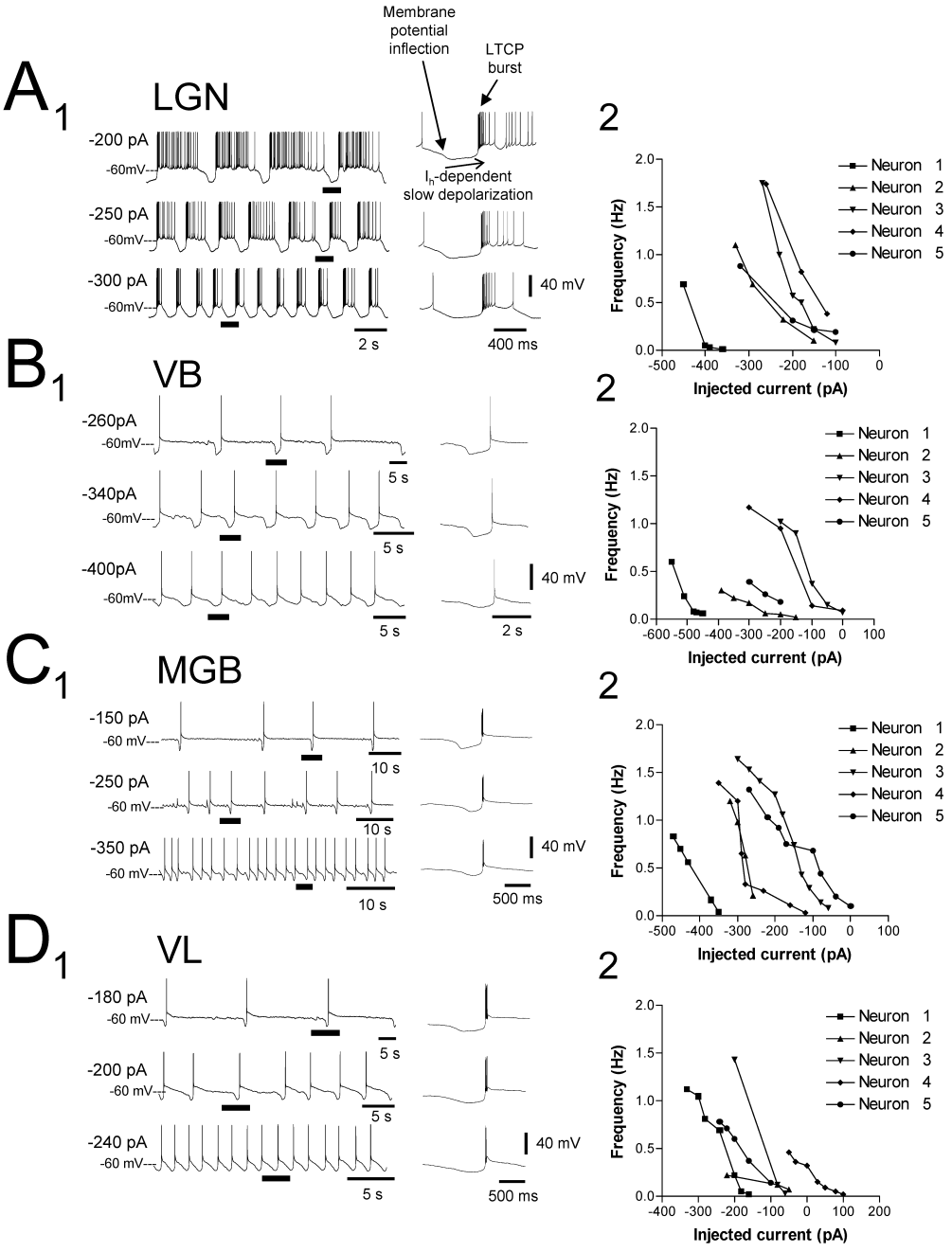

Figure 3. Comparison of the relationship between injected d.c. current and slow oscillation frequency in TC neurons of the cat LGN, VB, MGB and VL

A_1, B_1, C_1, and **D_1**. Examples of the slow oscillation in TC neurons of the cat LGN, VB, MGB and VL, respectively, at different levels of injected d.c. current as indicated. All underlined sections are expanded on the right and indicate an invariance of the DOWN state with respect to membrane polarization (see also Fig. $6A_3$ and $6B_3$). Note that in all cases, i) the UP state of the slow oscillation commences with an LTCP burst, ii) the UP to DOWN state transition is marked by a clear membrane potential inflection, and iii) the DOWN state is shaped by a slow, I_h-dependent depolarization (Hughes et al., 2002b). **A_2-D_2**. Plots showing the relationship between slow oscillation frequency and injected d.c. current for 5

different neurons in each nucleus. The traces in **A_1-D_1** correspond to neurons 5, 2, 4 and 5 in the respective plots. Note how the vast majority of neurons only exhibit a slow oscillation for negative steady d.c. current values.

Europe PMC Funders Author Manuscripts

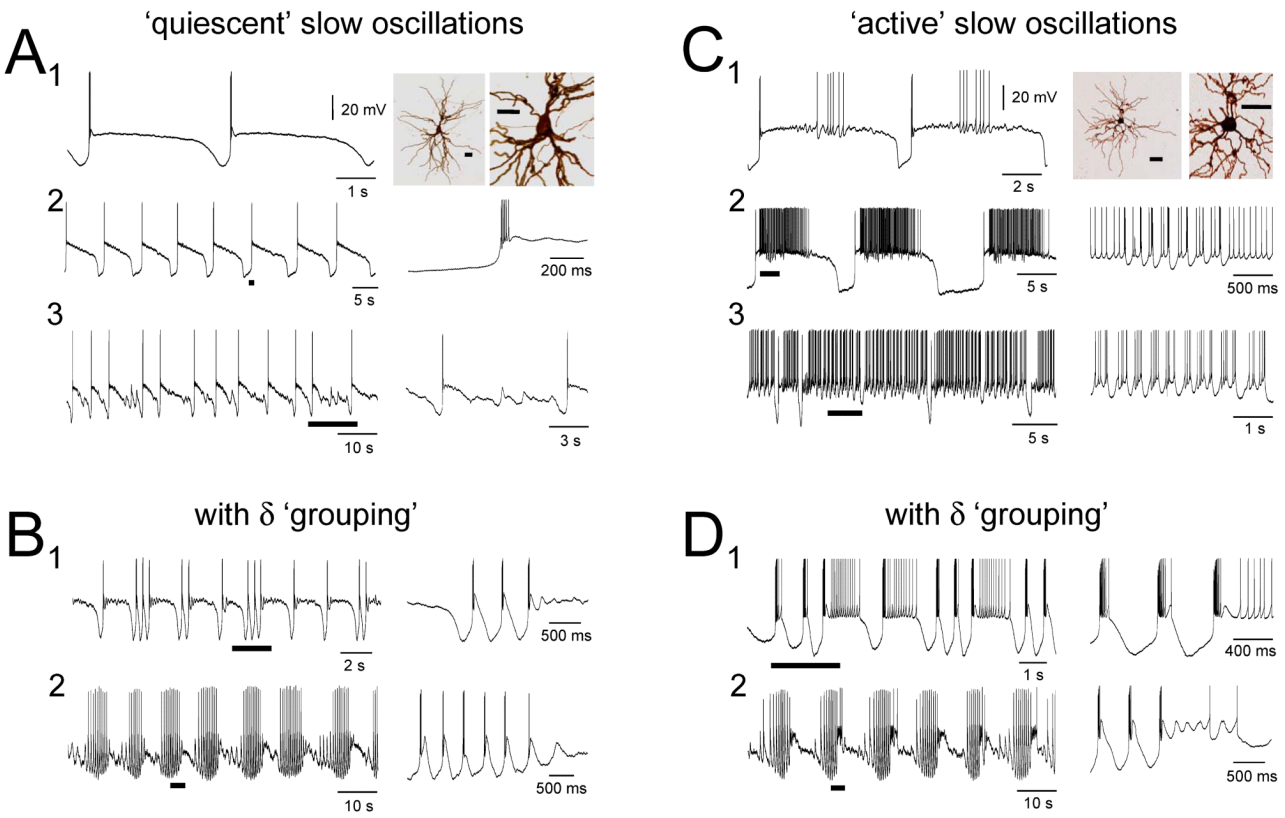

Figure 4. TC neurons of the cat LGN express the slow oscillation with striking and extensive heterogeneity

A. Different manifestations of the basic 'quiescent' slow oscillation in cat LGN TC neurons. The morphology of the neuron in $\mathbf{A_1}$ is shown to the right and further expanded on the far right. In $\mathbf{A_2}$ and $\mathbf{A_3}$ the underlined sections are expanded to the right. **B**. 'Quiescent' slow oscillations in cat LGN TC neurons showing either brief (**1**) of more extensive (**2**) 'grouped' δ sequences. In $\mathbf{B_1}$ and $\mathbf{B_2}$ the underlined sections are expanded to the right. **C**. Different manifestations of the basic 'active' slow oscillation in cat LGN TC neurons exhibiting UP states comprising either tonic firing only (**1**), a mixture of tonic firing and HT bursts (**2**) or HT bursts only (**3**). The morphology of the neuron in $\mathbf{C_1}$ is shown to the right and further expanded on the far right. Note the smaller soma size compared to that shown in $\mathbf{A_1}$. In $\mathbf{C_2}$ and $\mathbf{C_3}$ the underlined sections are expanded to the right **D**. 'Active' slow oscillations in cat LGN TC neurons showing either brief (**1**) of more extensive (**2**) 'grouped' δ sequences. In $\mathbf{D_1}$ and $\mathbf{D_2}$ the underlined sections are expanded to the right. Note that for 'grouped' oscillations the slow, I_h-dependent depolarization is evident between each LTCP-mediated burst. All recordings are from different cells. (All scale bars are 50 μm).

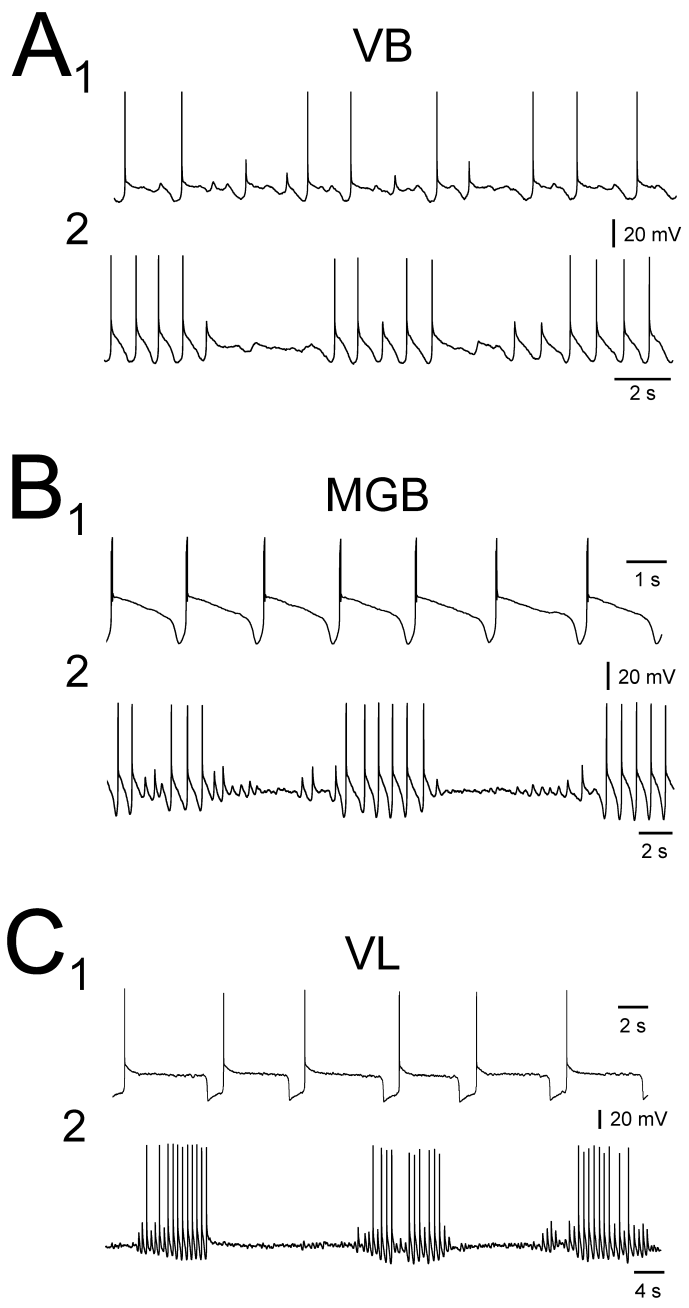

Figure 5. Restricted expression of the slow oscillation in TC neurons of the cat VB, MGB and VL

A, B and C, Representative examples of slow oscillations recorded intracellularly from the cat VB, MGB and VL, respectively. In these nuclei, all oscillations except one (see Fig. 6B) were of the 'quiescent' type. The second example in each panel is of an oscillation that also exhibits δ 'grouping'. All recordings are from different cells.

Europe PMC Funders Author Manuscripts

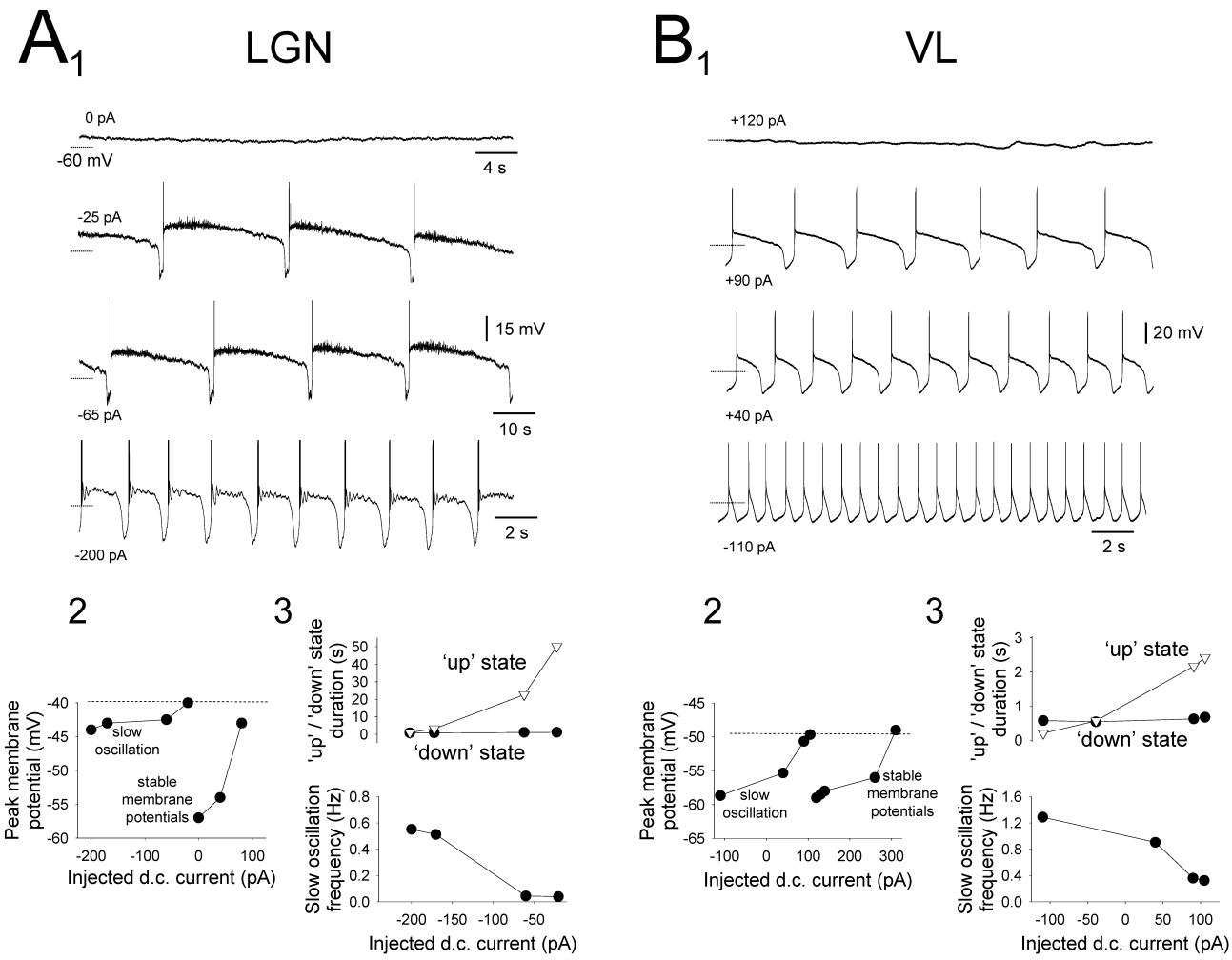

Figure 6. Specific properties of the 'quiescent' slow oscillation in cat TC neurons

A_1. Changes in the activity of a cat LGN TC neuron exhibiting a 'quiescent' slow oscillation without δ 'grouping' in response to variations in injected d.c. current. Note the characteristic increase in frequency that occurs with hyperpolarization. **A_2**. Plot showing the peak membrane potentials evident at different levels of injected current. Note that the maximum level of depolarization generated by the UP state (dotted lines) is greater than a range of stable membrane potentials displayed by this neuron when it is subjected to more steady depolarizing current and, specifically, is larger than the resting membrane potential of this neuron (i.e. at 0 pA). **A_3**. Plots showing the variation in UP (∇) and DOWN (•) state duration (top) and slow oscillation frequency (bottom) with respect to injected d.c. current, confirming that changes in frequency occur almost exclusively through a variation in the UP state duration. **B_1**. Changes in the activity of a cat VL TC neuron exhibiting a 'quiescent' slow oscillation without δ 'grouping' in response to variations in injected d.c. current. **B_2**. Plot showing the peak membrane potentials evident at different levels of injected current. As in the neuron shown in **A**, the UP state generates levels of depolarization which can be greater than some of the stable membrane potential levels reached by this neuron when it is subjected to more steady depolarizing injected current than during the slow oscillation. **B_3**. Plots showing the variation in UP (∇) and DOWN (•) state duration (top) and slow

oscillation frequency (bottom) with respect to injected d.c. current. Again, this confirms that changes in frequency occur almost entirely through a variation in the UP state duration. Note the more depolarized membrane potentials reached during the UP state of the LGN slow oscillation shown in **A_2** compared with those from the VL in **B_2** (see Table 1).

Europe PMC Funders Author Manuscripts

Europe PMC Funders Author Manuscripts

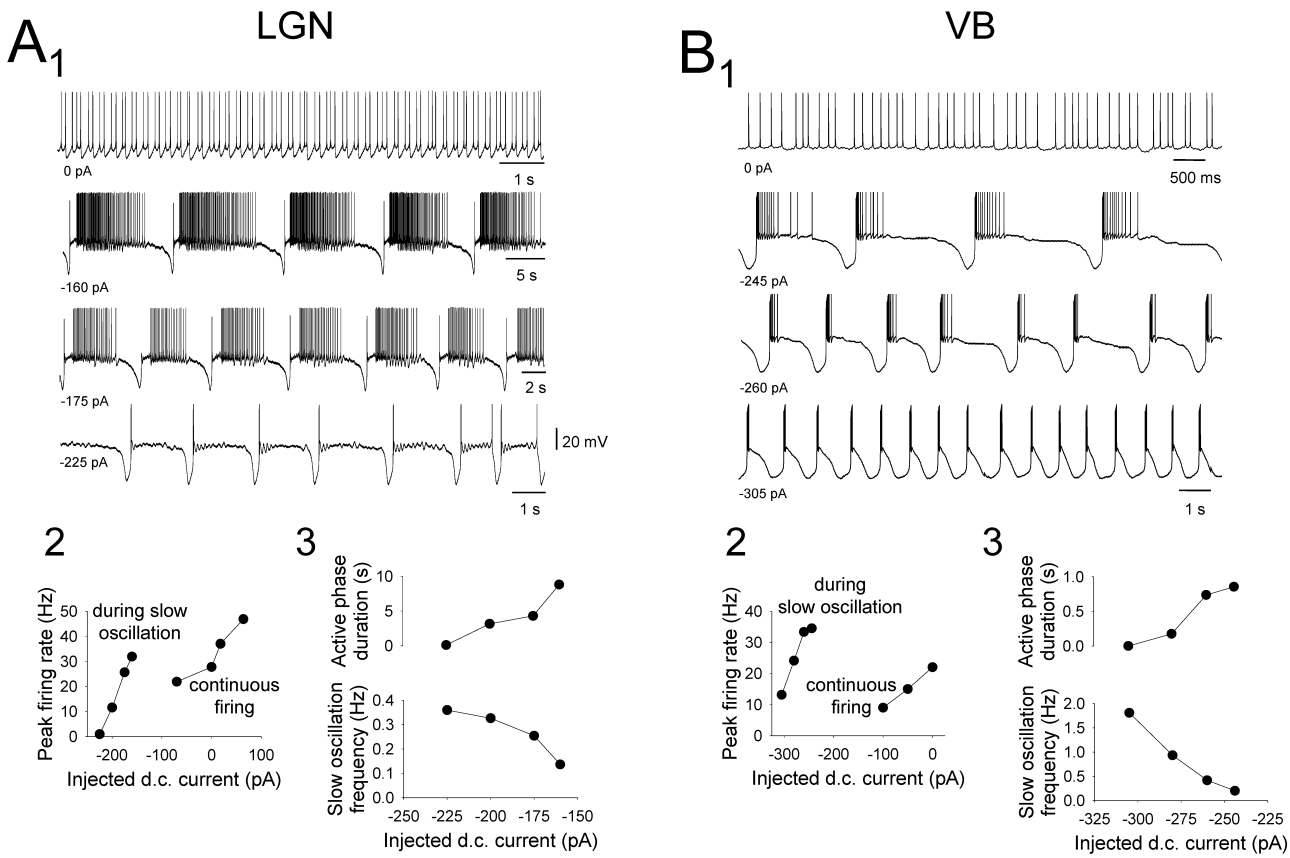

Figure 7. Specific properties of the 'active' slow oscillation in cat TC neurons

A_1. Changes in the activity of a cat LGN TC neuron exhibiting an 'active' slow oscillation in response to variations in injected d.c. current. Note also the almost complete lack of UP state firing when the slow oscillation is at its fastest in the bottom trace **A_2**. Plot showing the peak firing rate evident at different levels of injected current. For the slow oscillation this indicates the degree of excitation generated by the UP state (see methods). Note that the UP state can support more intense firing than is present when the neuron fires continuously in response to greater amounts of steady injected current. **A_3**. Plots showing the variation in the duration of the 'active' phase (top) and slow oscillation frequency (bottom) with respect to injected current. **B_1**. Changes in the activity of a cat VB TC neuron exhibiting an 'active' slow oscillation in response to variations in injected d.c. current. **B_2**. Plot showing the peak firing rate evident at different levels of injected current. Again, note that the UP state can support more intense firing than is present when the neuron fires continuously in response to greater amounts of steady current. **B_3**. Plots showing the variation in the duration of the 'active' phase (top) and slow oscillation frequency (bottom) with respect to injected current. Note that the extent to which additional firing occupies the UP state in the VB oscillation shown in **B_2** is noticeably less than for the LGN case shown in **A_2** (see also Figs. 4C and 4D).

Europe PMC Funders Author Manuscripts

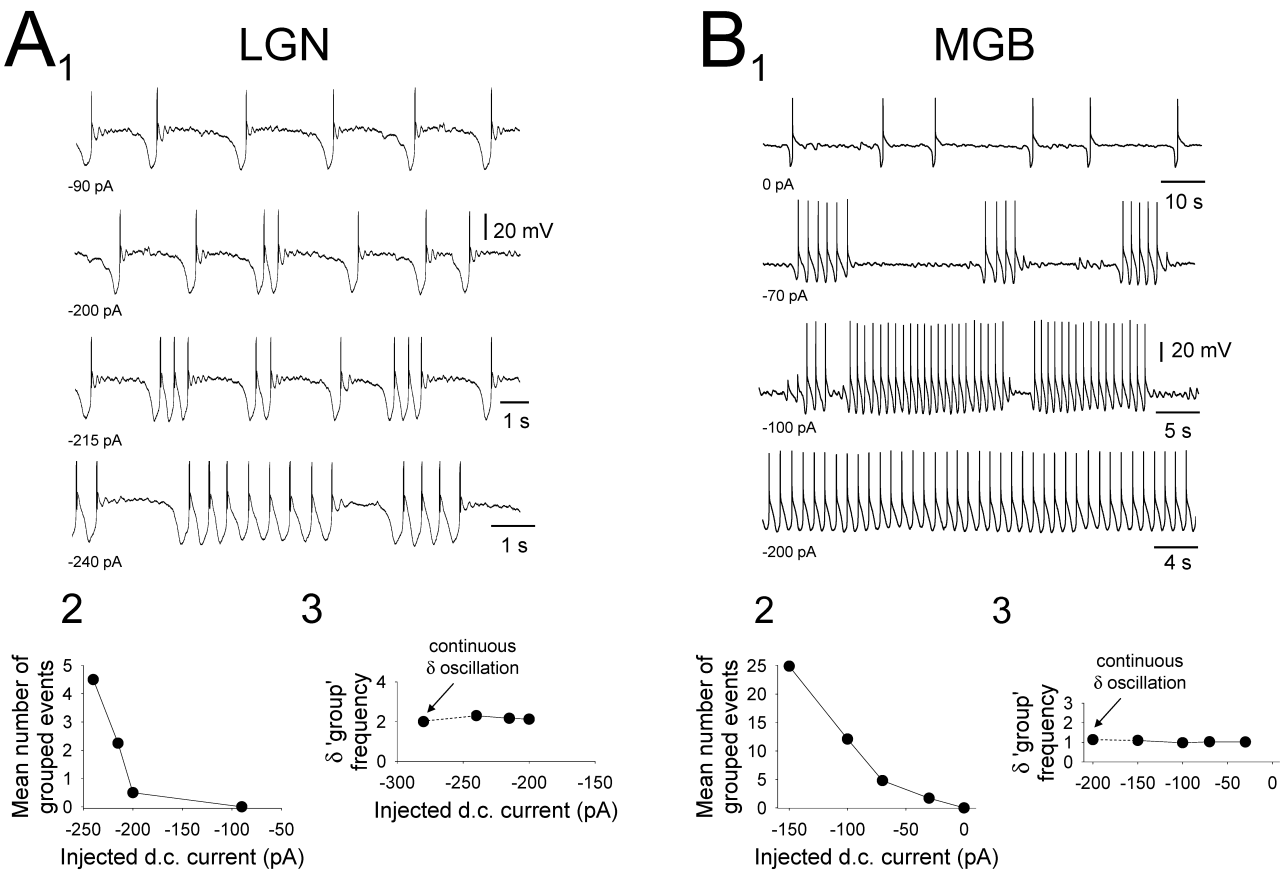

Figure 8. Specific properties of 'grouped' δ oscillations in cat TC neurons

A_1. Changes in the activity of a cat LGN TC neuron exhibiting a 'grouped' δ 'quiescent' slow oscillation in response to variations in injected d.c. current. **A_2**. Plot showing the change in the mean number of 'grouped' events with respect to injected current. **A_3**. Plot showing the variation in the mean interburst frequency of δ sequences with respect to injected d.c. current. Note that the frequency of δ activity remains relatively stable as injected current is altered. **B_1**. Changes in the activity of a cat MGB TC neuron exhibiting a 'grouped' δ 'quiescent' slow oscillation in response to variations in injected d.c. current. Note how 'grouped' δ oscillations occur between a 'pure' slow oscillation (top trace) and a continuous δ oscillation (bottom trace). **B_2**. Plot showing the change in the mean number of 'grouped' events with respect to injected current. **B_3**. Plot showing the variation in the mean interburst frequency of δ sequences with respect to injected d.c. current. Again, note that the frequency of δ activity remains relatively stable as injected current is varied.

Europe PMC Funders Author Manuscripts

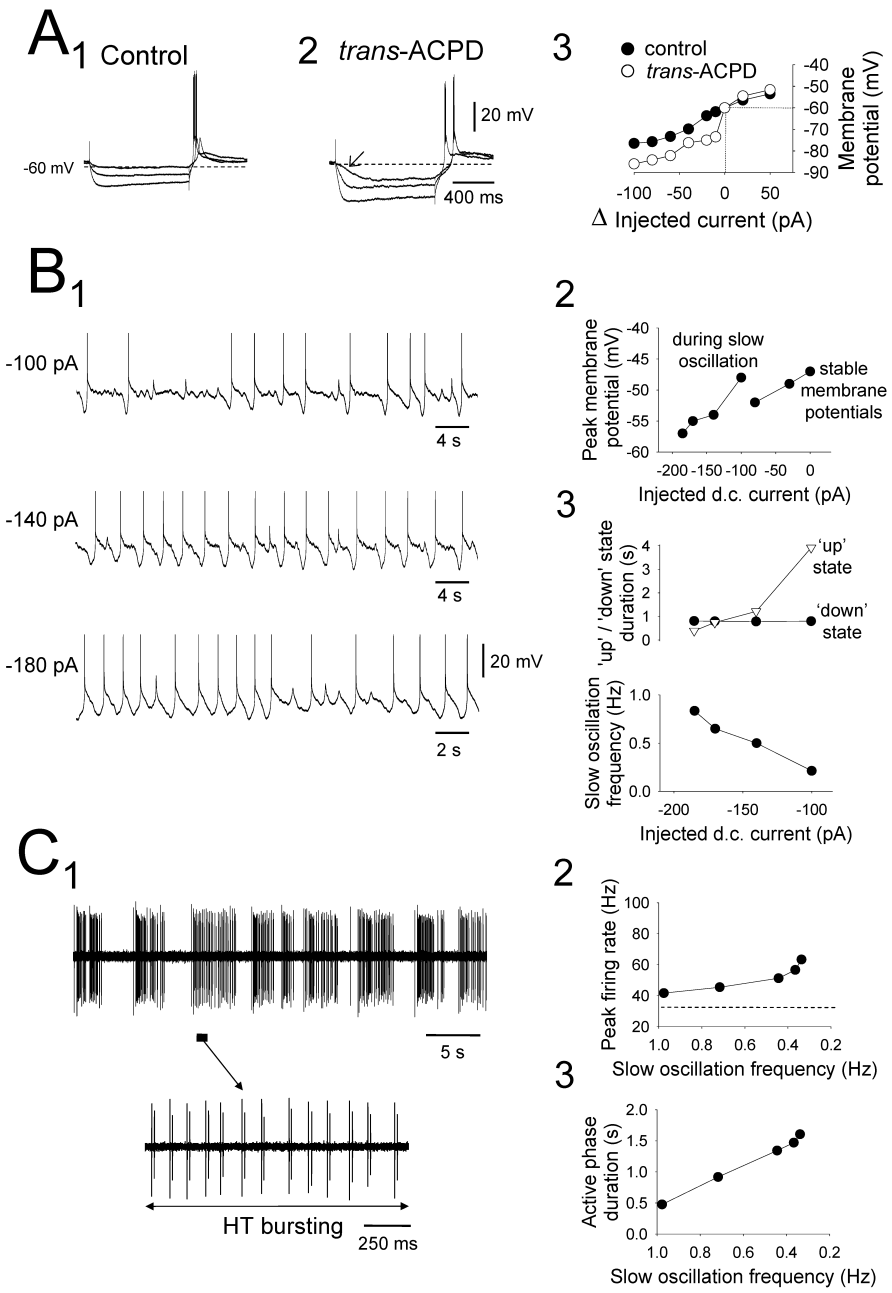

Figure 9. Intra- and extracellular recordings of the slow oscillation in the rat LGN

A_1 and **A_2**. Voltage response of a rat LGN TC neuron to a range of injected current steps before (**1**) and after (**2**) *trans*-ACPD application. Note the appearance of a distinctly non-linear membrane charging pattern in **A_2** which encompasses an inflection point (↙). *Trans*-ACPD also led to a slow oscillation in this neuron (shown in Supp. Fig. 4A). **A_3**. Relationship between changes in injected d.c. current and membrane potential for the neuron depicted in **A_1** and **A_2**. **B_1**. Changes in the activity of a different rat LGN TC neuron exhibiting a 'quiescent' slow oscillation in response to variations in injected d.c. current. **B_2**. Plot showing the peak membrane potentials evident at different levels of injected current.

Note that the UP state can generate a level of depolarization which is greater than a range of stable membrane potentials reached when the neuron is subject to more injected current. **B_3**. Plots showing the variation in UP (∇) and DOWN (•) state duration (top) and slow oscillation frequency (bottom) with respect to injected d.c. current. Note that the change in frequency occurs almost exclusively through a variation in the UP state duration. **C_1**. 'Active' slow oscillation the rat LGN comprising additional firing which is predominantly composed of HT bursting (see expanded section below). **C_2**. Plot showing the peak rates of firing at different frequencies of the slow oscillation shown in **C_1**. The dotted line represents the mean rate of continuous firing in the presence of 100 μM *trans*-ACPD (see Supplementary Information for further details). **C_3**. Plot illustrating the alteration in the duration of the active phase that occurs as the frequency of the slow oscillation changes.

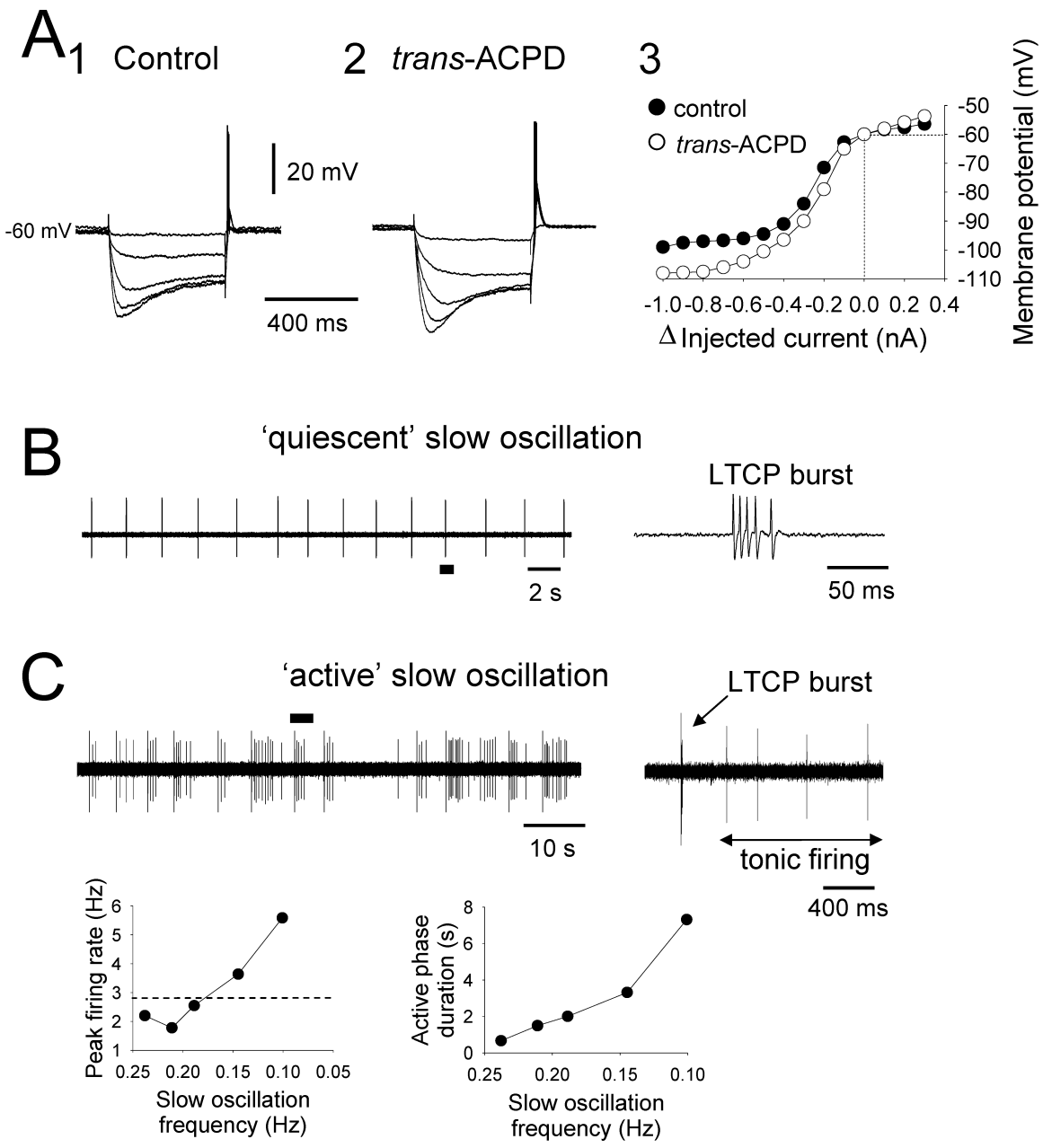

Figure 10. Intra- and extracellular recordings from the mouse LGN

A_1 and **A_2**. Voltage response of a mouse LGN TC neuron to injected current steps before and after *trans*-ACPD application. Note the lack of non-linear membrane charging pattern and inflection point in **A_2**. **A_3**. Relationship between changes in injected d.c. current and membrane potential for the neuron depicted in **A_1** and **A_2**. **B.** Extracellular recording in the mouse LGN exhibiting a basic 'quiescent' slow oscillation. The underlined LTCP-mediated burst is expanded on the right. **C**. 'Active' slow oscillation in the mouse LGN comprising additional firing which is solely composed of single spikes (see expanded section on the right). The lower left plot shows the peak rates of additional firing for different frequencies

of the slow oscillation. The dotted line represents the mean rate of continuous firing in the presence of 100 μM *trans*-ACPD (see Supplementary Information for further details). The right plot illustrates the alteration in the duration of the 'active' phase that occurs as the slow oscillation changes frequency. Note that no TC neurons recorded extracellularly in the mouse thalamus exhibited 'active' UP states composed solely of HT bursts.

Europe PMC Funders Author Manuscripts

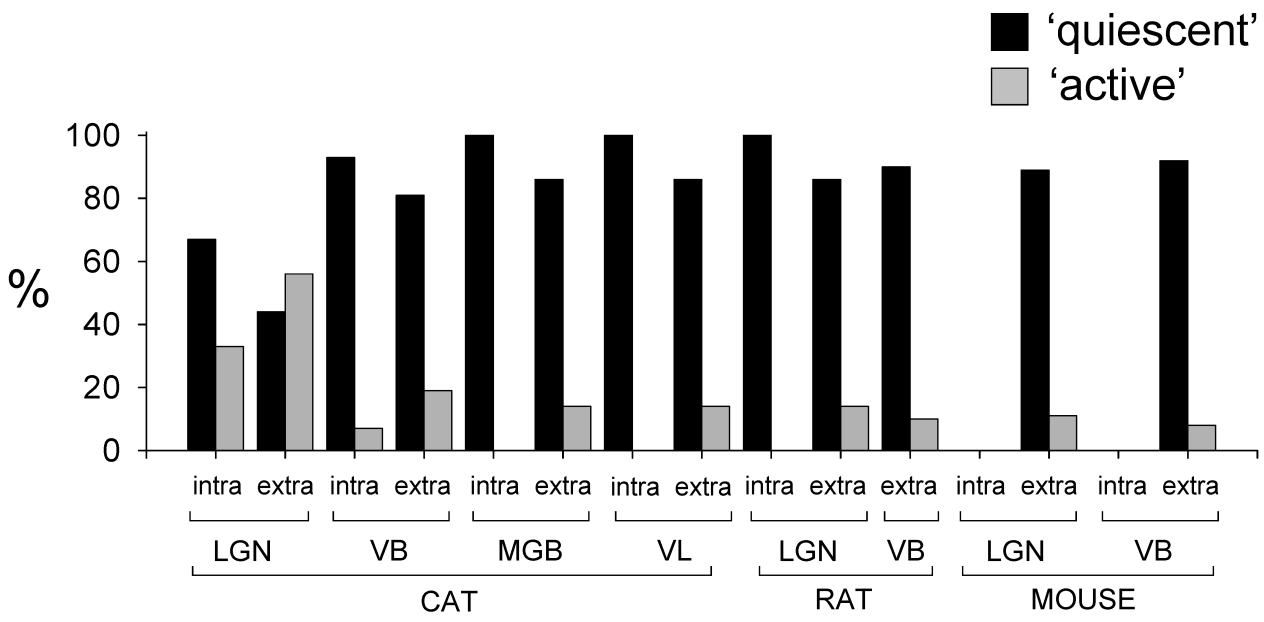

Figure 11. Summary of the prevalence of different types of slow oscillation in TC neurons of different nuclei and species

Percentages of ‘quiescent’ (black bars) and ‘active’ (gray bars) slow oscillations observed with intra- and extracellular recordings in each nucleus examined. Note the high proportion of ‘active’ oscillations in the cat LGN compared to all other nuclei. This especially evident in extracellular recordings where ‘active’ oscillations are more prevalent than ‘quiescent’ ones.

Europe PMC Funders Author Manuscripts

Europe PMC Funders Author Manuscripts

Table 1

Comparison of the properties of the slow oscillation in TC neurons of different thalamic nuclei of various species assessed with intracellular recordings.

% is the percentage of neurons exhibiting a slow oscillation.

							'Quiescent' slow oscillations		'Active' slow oscillations				δ 'grouping'	
		%	R_N of oscillating neurons (MΩ)	Min. freq. (Hz)	UP state duration (s)	DOWN state duration (s)	V_m† (mV)	UP state peak (mV)	Spont. tonic firing freq. (Hz)†	Max. peak tonic firing freq. (Hz)	Spont. HT burst freq. (Hz)†	Max. peak HT burst freq. (Hz)	Max. no. of 'grouped' δ events	'Grouped' δ freq. (Hz)
CAT	LGN	60	614.2± 92.6 (n=34)	0.30±0.04 (n=34)	1.4±0.2 to 11.3±2.4 (n=26)	1.0±0.2 to 1.4±0.2 (n=26)	-52.2±0.4 (n=15)	-48.3±0.7 (n=23) p<0.01†††	10.2±1.2 (n=7)	11.6±3.4 (n=7)	6.7±1.1 (n=3)	6.5±1.2 (n=3)	5.5±1.1 (n=9)	1.7±0.2 (n=9)
	VB	54	758.6± 255.2 (n=12)	0.12±0.04 (n=11)	1.5±0.4 to 14.1±5.6 (n=8)	1.0±0.2 to 1.2±0.2 (n=8)	-55.6±0.8 (n=8)	-56.1±1.8 (n=11) p<0.01††	12.6 (n=1)	23.6 (n=1)			7.2±1.0 (n=4)	1.6±0.1 (n=4)
	MGB	56	723.1± 151.9 (n=14)	0.06±0.03 (n=14) p<0.01††	2.3±0.6 to 17.1±3.7 (n=7)	0.9±0.1 to 1.4±0.2 (n=7)	-55.2±0.6 (n=10)	-54.7±1.4 (n=14) p<0.01††					10.8±5.3 (n=7) p<0.01††	1.2±0.1 (n=7)
	VL	73	766.7± 272.5 (n=8)	0.04±0.02 (n=8) p<0.01††	3.9±1.3 to 48.5±14.2 (n=6)	1.2±0.2 to 1.3±0.3 (n=6)	-55.7±0.7 (n=7)	-53.3±1.6 (n=8) p<0.01††					15.4±3.2 (n=2) p<0.01††	1.4±0.1 (n=2)
RAT	LGN	40	1040.0± 272.6 (n=4)	0.25±0.05 (n=4)	1.0±0.2 to 6.7±2.1 (n=4)	0.8±0.02 to 0.8±0.03 (n=4)	-57.4±0.7 (n=4)	-57.6±0.8 (n=4) p<0.01††						

†in the absence of injected d.c. current when most (see Fig. 3 and text) neurons are depolarized above the region where the slow oscillation occurs and exhibit a stable resting membrane potential.

††compared to the cat LGN.

†††compared to mean V_m. As stated in the text, no mouse TC neurons displayed a slow oscillation when assessed with intracellular recordings.